

# Multimodal Learning To Improve Segmentation With Intraoperative CBCT & Preoperative CT

Maximilian E. Tschuchnig<sup>1,2</sup>[0000-0002-1441-4752], Philipp Steininger<sup>3</sup>, and Michael Gadermayr<sup>1</sup>[0000-0003-1450-9222]

<sup>1</sup> Salzburg University of Applied Sciences  
`{firstname,lastname}@fh-salzburg.ac.at`

<sup>2</sup> University of Salzburg

<sup>3</sup> MedPhoton GmbH

**Abstract.** Intraoperative medical imaging, particularly Cone-beam computed tomography (CBCT), is an important tool facilitating computer aided interventions, despite a lower visual quality. While this degraded image quality can affect downstream segmentation, the availability of high quality preoperative scans represents potential for improvements. Here we consider a setting where preoperative CT and intraoperative CBCT scans are available, however, the alignment (registration) between the scans is imperfect. We propose a multimodal learning method that fuses roughly aligned CBCT and CT scans and investigate the effect of CBCT quality and misalignment (affine and elastic transformations facilitating misalignment) on the final segmentation performance. As an application scenario, we focus on the segmentation of liver and liver tumor semantic segmentation and evaluate the effect of intraoperative image quality and misalignment on segmentation performance. To accomplish this, high quality, labelled CTs are defined as preoperative and used as a basis to simulate intraoperative CBCT. We show that the fusion of preoperative CT and simulated, intraoperative CBCT mostly improves segmentation performance and that even clearly misaligned preoperative data has the potential to improve segmentation performance.

**Keywords:** Multimodal Learning · Radiology · Intraoperative · Segmentation

## 1 Introduction

Intraoperative medical imaging is an important tool for computer aided intervention. Mobile robotic medical imaging systems like cone-beam computed tomography (CBCT) [11], enable intraoperative medical imaging with real time capabilities. CBCT is an imaging method that utilizes a cone-shaped X-ray beam and a flat-panel detector to capture detailed, three-dimensional images of a patient’s anatomy using a mobile system [8]. However, rapid intraoperative imaging often comes with the disadvantage of significantly lower image quality, in turn affecting the performance of downstream tasks like segmentation.

While the degraded image quality of CBCT scans can affect downstream segmentation, the availability of high quality preoperative scans represents a high potential for improvements based on the idea of multi-modal learning. Multi-modal learning is an approach that involves fusing images from multiple domains to improve machine learning models for a downstream task like segmentation. In medical imaging, a common approach is to enrich computed tomography (CT) data, focusing on bone structures with Magnetic Resonance (MR) data for soft tissue analysis [15,10]. Multimodal learning is typically separated into three fusion strategies [15,14]: early, late and hybrid. The most common multimodal fusion, early-fusion, combines images of different modalities before being processed by a downstream model. Typically, the two domains are fused along a dimension additional to the spacial volume dimensions. Following this the fused images are processed jointly [15,12]. Another form of early fusion processes the volumes of different modalities in separate feature extraction stages, finally fusing the extracted features. In the case of segmentation using unet, this early-middle-fusion corresponds to multiple encoders, fusion of these encoders in the latent space and a shared decoder. Late-fusion is performed before the final layer of the downstream task. In a segmentation case, late-fusion merges the features extracted from multiple independent encoder-decoder networks before final segmentation. Hybrid-fusion, combines aspects of both early and late fusion for enhanced performance.

Typically, multimodal learning assumes that the fused images are aligned, utilizing affine or even elastic registration. Particularly, deep learning-based approaches[2,4] have shown promising performance. However, registration of 3D samples, if performed accurately on a high resolution, is computationally expensive, especially non-linear deformations. Podobnik et al. [10] integrated registration within their hybrid multimodal segmentation approach by merging features from different modality branches using the affine Spatial Transformer Networks (STN) localization net [7], along with a grid generator and sampler.

Here we consider the setting where preoperative CT scans and intraoperative CBCT scans are available, however, the alignment (registration) between the scans is imperfect. We hypothesised that, by adding high quality, preoperative CTs to our intraoperative CBCTs, segmentation performance will increase. We assume that, the more accurate the alignment between the modalities is, the more pronounced the performance increase will be.

**Contribution:** We propose a method that combines roughly aligned CBCT and CT scans (early-fusion) and investigate the effect of CBCT quality and misalignment (based on affine and elastic transformations) on the final segmentation performance.

In detail, we synthesised a collection of synthetic CBCT data, focusing on the segmentation of liver and liver tumors based on the LiTS CT dataset [3]. Beyond varying the amount of digitally reconstructed radiographs (DRR) used for CBCT synthesis, resulting in 5 different imaging qualities, we generated 9 variably misaligned versions based on linear and non-linear models and 1 baseline model resulting in overall 50 sub data sets. We evaluated all 45 combinations

based on a Unet architecture and compared the performances to unimodal processing of the 5 baseline data combinations.

## 2 Methods

We propose to fuse intraoperative CBCT with high quality, preoperative CT to investigate if this kind of additional information improves model training for computer aided intervention systems. To accomplish this study we apply multimodal learning in medical imaging for the downstream task of liver and liver tumor segmentation using CT and CBCT data based on the LiTS dataset [3]<sup>4</sup>. Similar to Ren et al. [12] we used early-fusion for the multimodal setup. Furthermore, we investigated two parameters,  $\alpha_{np}$  as the number of DRRs used to simulate the current CBCT, and  $\alpha_a$  as the current strength of the alignment between the preoperative CT and the intraoperative CBCT. Mean dice of the CBCT segmentation targets of either liver or liver tumor over 4 repetitions of each experiment was used as the evaluation metric. As a baseline, segmentation was performed using the CBCT unimodal, which was evaluated for all possibilities of  $\alpha_{np}$ , leading to 100 different experiments overall. Misaligned was performed using affine transformations during training and validation to decrease loading times in the dataloader and affine followed by elastic transformations for testing to account for non-linear deformations.

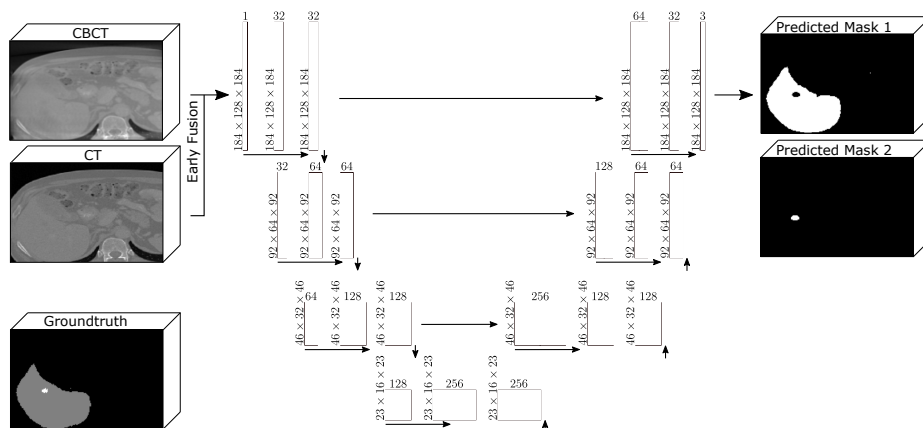


**Fig. 1.** Multimodal model configuration. Additionally to using the intraoperative CBCT, the model also took preoperative CT in an early fusion multimodal setup. This data was processed by the given unet, segmenting liver and liver tumors.

We used a holistic, 3D-Unet similar to Tschuchnig et al. [13] as our segmentation model and our baseline for all possible  $\alpha_{np}$  and adapted it for multimodality

<sup>4</sup> For the CBCT version of LiTS see the Kaggle dataset *CBCT Liver and Liver Tumor Segmentation Train Data*

by adding a paired and more or less aligned ( $\alpha_a$ ), preoperative CT as a second channel, resulting in a 4d data structure. The 3D-Unet used for segmentation, shown in Fig. 1, consisted of an encoder with 3 double convolution layers and  $3 \times 3 \times 3$  convolutional kernels, connected by 3D max pooling. The latent space was constructed using one double convolution block leading into the unet decoder, mirroring the encoder. As is typical for unet, each double convolutional output in the encoder was also connected to the decoder double convolutional block of the same order. Additionally, one 3D convolutional layer was added to the decoder with a filter size of  $1 \times 1 \times 1$  and the number of filters set to the amount of segmentation classes (in the case of liver and liver tumor segmentation this value was set to 2). The number of feature maps were set to  $\{32, 64, 128, 256\}$  as shown in the figure. Batch norm was applied after each layer in the double convolutional blocks. The model was trained utilizing a sum of binary cross-entropy and Dice similarity. For our baseline, a unimodal Unet was used, with only the CBCT as input. Our multimodal approach added the high quality, misaligned and preoperative CT as a second channel to the CBCT.

## 2.1 Experimental Details

All models were trained on an Ubuntu server using 3 NVIDIA RTX A6000 graphics cards. Due to the large size of the data and memory restrictions (48 GB VRAM), the volumes were downscaled (isotropic) by the factor of two. To binarize the masks, a threshold of 0.5 was applied to each channel of the unet output. We investigated the effect of 1) changing CBCT quality by adapting  $\alpha_{np}$  and 2) changing of CT/CBCT alignment through  $\alpha_a$ . As an additional baseline, CBCT volumes with perfectly aligned CT,  $\alpha_a = 0$ , was also investigated. All experiments were trained and evaluated 4 times to facilitate stable results with the same random splits as well as the same random CT misaligned for comparable result. Adam was used as an optimizer with a learning rate of 0.005. Since annotations were not available for the LiTS test dataset, the test dataset was disregarded for this publication and the original train set was separated into training-validation-testing data [1,5]. The separation was performed using the splits training: 0.7, validation: 0.2, testing: 0.1.

## 2.2 Dataset Generation

For evaluation of the multimodal learning approach, paired CT and CBCT volumes had to be established and misalignment between CT and CBCT performed.

To generate CBCT/CT pairs we simulated DRRs from the CT volumes, with a variable amount of DRRs  $\alpha_{np} \in \{32, 64, 128, 256, 490\}$ . We then used these DRRs to simulate CBCTs with varying visual quality. Higher  $\alpha_{np}$  corresponded with better image quality, with 490 serving as the best visual CBCT quality and 32 as the lowest visual quality with a high amount of artifacts [13]. Fig. 2 shows these steps to convert the CT LiTS dataset into synthetic CBCT scans, centered around the liver. It also displays how corresponding CTs and masks were fitted to the shapes of the synthesised CBCTs.

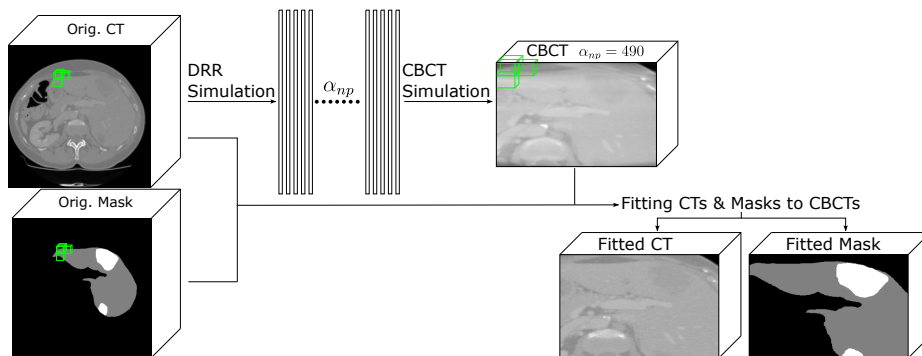


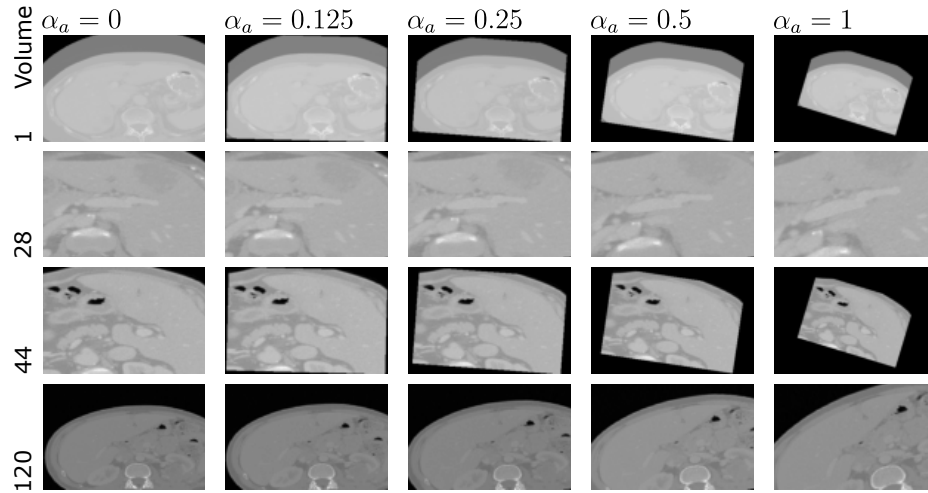
**Fig. 2.** Data generation process for synthetic CBCTs, corresponding masks and CTs. Using the LiTS CT data,  $\alpha_{np}$  DRRs were extracted and used to simulate CBCTs, centered around the liver. Further, CBCT voxel positions were mapped to the original CT and mask space, allowing for the generation of CTs and segmentation masks fitted to the synthesised CBCTs.

For evaluation of the multimodal learning approach, misalignment between the CTs and CBCTs was established. To decrease training and evaluation times only affine transformations were applied. During testing, these affine transformations were followed by elastic transformations to establish a more realistic scenario. Affine misalignment consisted of random scaling ( $[0.5, 1.5]$ , non-isotropic), rotation ( $[-22.5^\circ, 22.5^\circ]$ ), and translation ( $[0, 0.5]$ ) with linear interpolation. Elastic misalignment was applied with a maximum displacement of 20, 7 control points, no locked borders and linear image and nearest label interpolation. To reduce the amount of misaligned parameters to one, the augmentation factor  $\alpha_a \in \{0, 0.125, 0.25, 0.5, 1\}$  was introduced. This factor was multiplied with each of the augmentation methods maximum values, increasing the alignment effect through reducing  $\alpha_a$ . Augmentation was performed using torchio RandomAffine and RandomElasticDeformation.

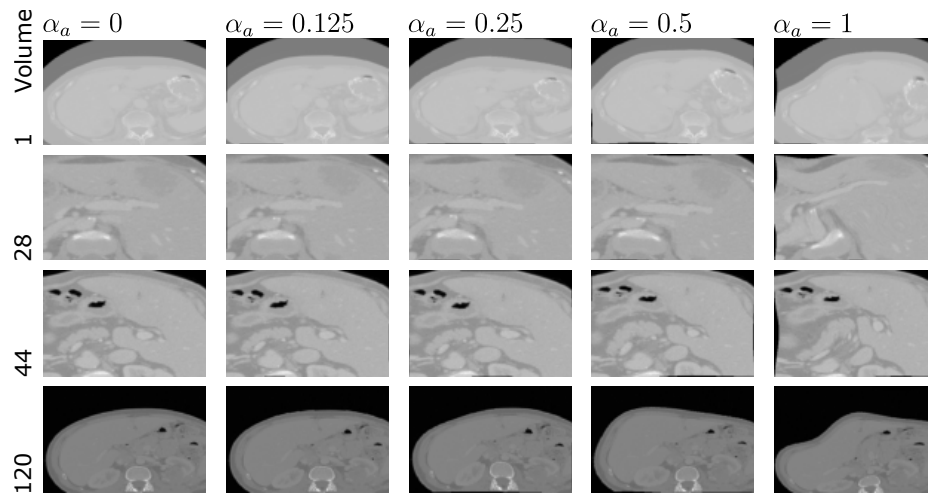
The LiTS dataset was chosen to perform the experiments [3]. LiTS consists of 131 abdominal CT scans in the training set and 70 test volumes. The 131 train volumes include segmentations of 1) the liver and 2) liver tumors. The dataset contains data from 7 different institutions with a diverse set of liver tumor diseases. The CTs were acquired using different CT scanners and acquisition protocols. For further information about the dataset we refer to Bilic et al. [3].<sup>5</sup>

Fig 3 shows results of affine augmentation with the augmentation strength from  $\alpha_a \in \{0, 0.125, 0.25, 0.5, 1\}$  and 4 different volumes. Fig 4 shows the same volumes, with applied random elastic transform. Here we display the elastics transformation in isolation for improved readability.

<sup>5</sup> To download the LiTS dataset follow the link: <https://competitions.codalab.org/competitions/17094>



**Fig. 3.** Results of the random affine augmentation with differing augmentation strengths  $\alpha_a \in \{0, 0.125, 0.25, 0.5, 1\}$  of 4 different volumes.



**Fig. 4.** Results of the random elastic augmentation with differing augmentation strengths  $\alpha_a \in \{0, 0.125, 0.25, 0.5, 1\}$  of 4 different volumes.

### 3 Results

Experimental results are shown in Table 1, denoted as mean Dice values. The test data was transformed using the introduced random affine transforms (affine) and the affine transformations followed by the introduced elastic transforms (elastic). Two baselines are also given (base) unimodal, with no preoperative CT (no ct) and perfect alignment (s0). Blue values show improvements to the baseline (no ct), while red values show worse results. If the values are bold there is at least a 5% increase/decrease. The +, - corresponds to improvements/decreases to the previous, less aligned experiments. If +, - are colored, the effect is bigger than 5%. The different  $\alpha_{np}$  are displayed horizontally and  $\alpha_a$  vertically for both liver and liver tumor segmentation. In the affine case, the results show an improvement to the baseline in all liver segmentation and in most liver tumor segmentation cases. The biggest improvement for liver segmentation was achieved with the parameters  $\alpha_{np} = 32$  and  $\alpha_a = 0$  with an improvement from 0.784 to 0.932 resulting in an increase of 0.148. For liver tumor segmentation, the biggest improvement was also achieved with the parameters  $\alpha_{np} = 32$  and  $\alpha_a = 0$  from 0.029 to 0.297 resulting in an increase of 0.268. There was also an observable trend of increasing dice scores from  $\alpha_a \in \{0.5, 0.25, 0.125, 0\}$ . This trend was stronger, the lower  $\alpha_{np}$  was. Adding elastic transformation on top of affine transformations lead to slightly worse results in the cases of  $\alpha_a \in 0.5, 0.25$  with  $\alpha_{a=0.25}$  suffering most from adding elastic transformations with an average dice decrease of 0.023 for liver and 0.032 for liver tumor segmentation. The elastic transformation effects regarding  $\alpha_{np}$  show a decrease of average Dice proportional to image quality. The most significant decrease in Dice, attributable to elastic transformation was reached with  $\alpha_{np} = 32$  with 0.016 for liver and 0.021 for liver tumor segmentation.

### 4 Discussion

The results confirmed the hypothesis that enriching intraoperative CBCT with roughly aligned preoperative CT can improve downstream tasks like segmentation. Most multimodal setups improved downstream performance with the only outliers observable in liver tumor segmentation with  $\alpha_a \in \{0.5, 1\}$  and  $\alpha_{np} \in \{490, 256, 128, 64\}$  and  $(\alpha_a, \alpha_{np}) = (0.25, 256)$  in the affine misaligned cases. If data was additionally misaligned using elastic transformations,  $(\alpha_a, \alpha_{np}) = (0.25, 490)$  also lead to a decrease in average dice.

Several trends are observable. For one, the worse the CBCT quality, the more can be gained by adding high quality CT, leading to an increase of Dice from  $0.784 \rightarrow 0.932$  for liver and  $0.029 \rightarrow 0.297$  for liver tumor segmentation. This is an especially important result since it clearly shows a positive effect to adding preoperative information to possibly low-quality interoperative CBCT. This effect is especially pronounced in the case of liver segmentation, where baseline scores can be reached using  $\alpha_{np} = 32$ .

**Table 1.** Experimental results (affine and elastic misalignment) given as mean dice values. Blue values denote improvements to the baseline (no ct), while red values show worse results. If the values are in bold there is at least a 5% increase/decrease. The +, - corresponds to improvements/decreases to the previous, lower aligned experiments. If +, - are colored, this effect is bigger than 5%. Values represented are the baselines (base) with no preoperative CT information (no ct) and perfect alignment (s0), affine misaligned (affine) and affine in combination with elastic misaligned (elastic).

	Liver Segmentation					Liver Tumor Segmentation				
	490	256	128	64	32	490	256	128	64	32
base										
no ct	0.884	0.884	0.859	0.817	0.784	0.165	0.162	0.093	0.061	0.029
s0	<b>0.933</b>	+ 0.931	+ <b>0.931</b>	+ <b>0.933</b>	+ <b>0.932</b>	+ <b>0.330</b>	+ <b>0.322</b>	+ <b>0.298</b>	+ <b>0.325</b>	+ <b>0.297</b>
affine										
s1	<b>0.906</b>	+ 0.897	+ 0.879	+ 0.857	+ 0.806	+ <b>0.154</b>	- 0.124	- 0.057	- 0.023	- 0.051
s0.5	<b>0.895</b>	- 0.891	- 0.875	- 0.863	+ <b>0.851</b>	+ <b>0.096</b>	- <b>0.098</b>	- 0.077	+ 0.056	+ <b>0.107</b>
s0.25	<b>0.904</b>	+ 0.906	+ 0.893	+ <b>0.883</b>	+ <b>0.883</b>	+ 0.181	+ 0.160	+ <b>0.163</b>	+ <b>0.169</b>	+ <b>0.171</b>
s0.125	<b>0.908</b>	+ 0.900	- 0.889	- <b>0.884</b>	+ <b>0.887</b>	+ 0.187	+ 0.166	+ <b>0.166</b>	+ <b>0.152</b>	- <b>0.185</b>
elastic										
s1	<b>0.907</b>	+ 0.897	+ 0.880	+ 0.857	+ 0.081	+ <b>0.153</b>	- 0.122	- 0.057	- 0.022	- 0.049
s0.5	<b>0.895</b>	- 0.891	- 0.870	- 0.845	- 0.800	+ <b>0.098</b>	- <b>0.103</b>	- 0.085	+ 0.029	+ 0.049
s0.25	<b>0.893</b>	- 0.898	+ 0.869	- 0.853	+ <b>0.846</b>	+ <b>0.154</b>	+ 0.142	+ 0.136	+ <b>0.129</b>	+ <b>0.122</b>
s0.125	<b>0.910</b>	+ 0.901	+ 0.891	+ <b>0.885</b>	+ <b>0.887</b>	+ <b>0.186</b>	+ 0.168	+ <b>0.163</b>	+ <b>0.151</b>	+ <b>0.168</b>

We also observe a trend regarding alignment of preoperative CT and intraoperative CBCT. At first, increased alignment lead to mostly worse average Dice for  $\alpha_a \in \{1, 0.5\}$  followed by a notable increase in average Dice for  $\alpha_a \in \{0.25, 0.125, 0\}$ . This trend was only observed for liver tumor segmentation. We hypothesise that this is the case due to heavily misaligned data interfering with the training process. This is especially the case for complex structures like tumors. Here, the model can ignore the higher quality but heavily misaligned CT but overfitt to better aligned CT data. However, further experiments to determine the reason for this should be performed. For now our findings suggest that if there is significant misaligned and the target is difficult, such as liver tumor segmentation, preregistration is crucial for successful multimodal learning.

Further observation stem from the ablation effects of adding elastic misalignment on top of affine misalignment. The addition of elastic misalignment lead to a proportional decrease in downstream segmentation depending on the factor  $\alpha_{np}$ . Therefore, the same elastic misalignment had more pronounced degrading effects on segmentation performance the worse the image quality got, hinting at a possible implicit registration effect that diminishes with image quality. Investigating the factor  $\alpha_a$ , elastic misalignment had no effect in the cases of  $\alpha_a \in \{1, 0.125\}$  with the average change  $< 0.005$ . However, in the cases of  $\alpha_a \in \{0.5, 0.25\}$  the effect of adding elastic misalignment was on average a decrease of 0.021. These insights hint at the deformation of  $\alpha_a = 1$  already being almost unfeasible to handle in the affine case, leaving the addition of elastic transform in these cases without effect. Since we also observed almost no effect in the cases of  $\alpha_a = 0.125$  we suspected that in these cases the elastic transform was negligible, in com-



parison to the affine misalignment. Interestingly, these performance gains show that the unet used for segmentation implicitly learned limited registration.

Although we only evaluated our results on unet, this form of multimodal learning should theoretically work on similar representation learning based networks, using similar building blocks, most importantly convolutional filters. However, further experiments are needed to investigate this assumption e.g. using the Segment Anything Model [9] or UNETR [6].

## 5 Conclusion

This study highlights the effectiveness of multimodal learning for downstream tasks, combining roughly aligned intraoperative CBCT with high quality, preoperative CT data. It further investigates how the different factors of volume quality and volume alignment influence the performance of a specific multimodal learning based model. Using the multimodal learning setup, improvements in segmentation accuracy, especially when CBCT volume quality was suboptimal, were reported suggesting that high-quality preoperative CT data can compensate for intraoperative CBCT limitations, as long as the data is roughly aligned with each other. Therefore, using this approach, clinicians could be supplied with more reliable information for surgical decision-making, particularly in real-time settings of computer-assisted intervention. Assuming preregistration, this underscores the practical applicability of the approach. We further showed that a simple 3D unet was able to learn limited, implicit registration.

Since evaluation was based on synthetic data with relatively simple misalignment and without preregistration useful next steps would be to evaluate using real, paired preoperative and intraoperative data as well as incorporating (pre)registration into the multimodal model.

**Acknowledgments.** This project was partly funded by the Austrian Research Promotion Agency (FFG) under the bridge project "CIRCUIT: Towards Comprehensive CBCT Imaging Pipelines for Real-time Acquisition, Analysis, Interaction and Visualization" (CIRCUIT), no. 41545455 and by the county of Salzburg under the project AIBIA.

**Disclosure of Interests.** The authors have no competing interests to declare that are relevant to the content of this article.

## References

1. Araújo, J.D.L., da Cruz, L.B., Diniz, J.O.B., Ferreira, J.L., Silva, A.C., de Paiva, A.C., Gattass, M.: Liver segmentation from computed tomography images using cascade deep learning. *Computers in Biology and Medicine* **140**, 105095 (2022)
2. Balakrishnan, G., Zhao, A., Sabuncu, M.R., Guttag, J., Dalca, A.V.: Voxelmorph: a learning framework for deformable medical image registration. *IEEE transactions on medical imaging* **38**(8), 1788–1800 (2019)

3. Bilic, P., Christ, P., Li, H., Vorontsov, E., Ben-Cohen, A., Kaissis, G., others, Menze, B.: The liver tumor segmentation benchmark (lits). *Medical Image Analysis* **84** (Feb 2023). <https://doi.org/10.1016/j.media.2022.102680>
4. Chen, J., Frey, E.C., He, Y., Segars, W.P., Li, Y., Du, Y.: Transmorph: Transformer for unsupervised medical image registration. *Medical image analysis* **82**, 102615 (2022)
5. Han, K., Liu, L., Song, Y., Liu, Y., Qiu, C., Tang, Y., Teng, Q., Liu, Z.: An effective semi-supervised approach for liver ct image segmentation. *IEEE Journal of Biomedical and Health Informatics* **26**(8), 3999–4007 (2022)
6. Hatamizadeh, A., Tang, Y., Nath, V., Yang, D., Myronenko, A., Landman, B., Roth, H.R., Xu, D.: Unetr: Transformers for 3d medical image segmentation. In: *Proceedings of the IEEE/CVF winter conference on applications of computer vision*. pp. 574–584 (2022)
7. Jaderberg, M., Simonyan, K., Zisserman, A., et al.: Spatial transformer networks. *Advances in neural information processing systems* **28** (2015)
8. Jaffray, D.A., Siewerdsen, J.H., Wong, J.W., Martinez, A.A.: Flat-panel cone-beam computed tomography for image-guided radiation therapy. *International Journal of Radiation Oncology\* Biology\* Physics* **53**(5), 1337–1349 (2002)
9. Kirillov, A., Mintun, E., Ravi, N., Mao, H., Rolland, C., Gustafson, L., Xiao, T., Whitehead, S., Berg, A.C., Lo, W.Y., et al.: Segment anything. In: *Proceedings of the IEEE/CVF International Conference on Computer Vision*. pp. 4015–4026 (2023)
10. Podobnik, G., Strojan, P., Peterlin, P., Ibragimov, B., Vrtovec, T.: Multimodal ct and mr segmentation of head and neck organs-at-risk. In: *International Conference on Medical Image Computing and Computer-Assisted Intervention*. pp. 745–755 (2023)
11. Rafferty, M.A., Siewerdsen, J.H., Chan, Y., Daly, M.J., Moseley, D.J., Jaffray, D.A., Irish, J.C.: Intraoperative cone-beam ct for guidance of temporal bone surgery. *Otolaryngology—Head and Neck Surgery* **134**(5), 801–808 (2006)
12. Ren, J., Eriksen, J.G., Nijkamp, J., Korreman, S.S.: Comparing different ct, pet and mri multi-modality image combinations for deep learning-based head and neck tumor segmentation. *Acta Oncologica* **60**(11), 1399–1406 (2021)
13. Tschuchnig, M.E., Coste-Marin, J., Steininger, P., Gadermayr, M.: Multi-task learning to improve semantic segmentation of cbct scans using image reconstruction. In: *BVM Workshop*. pp. 243–248 (2024)
14. Zhang, Y., Yang, J., Tian, J., Shi, Z., Zhong, C., Zhang, Y., He, Z.: Modality-aware mutual learning for multi-modal medical image segmentation. In: *Medical Image Computing and Computer Assisted Intervention—MICCAI 2021: 24th International Conference, Strasbourg, France, September 27–October 1, 2021, Proceedings, Part I 24*. pp. 589–599 (2021)
15. Zhang, Y., Sidibé, D., Morel, O., Mériaudeau, F.: Deep multimodal fusion for semantic image segmentation: A survey. *Image and Vision Computing* **105**, 104042 (2021)